Electronic and Magnetic Properties of α-Keggin Anions: A DFT Study of [XM$_{12}$O$_{40}$]$^{n-}$, (M = W, Mo; X = Al^{III}, Si^{IV}, P^{V}, Fe^{III}, Co^{II}, Co^{III}) and [SiM$_{11}$VO$_{40}$]$^{m-}$ (M = Mo and W)

Joan Miquel Maestre,[†] Xavier Lopez,[†] Carles Bo,[†] Josep-M. Poblet,*,[†] and Nieves Casañ-Pastor[‡]
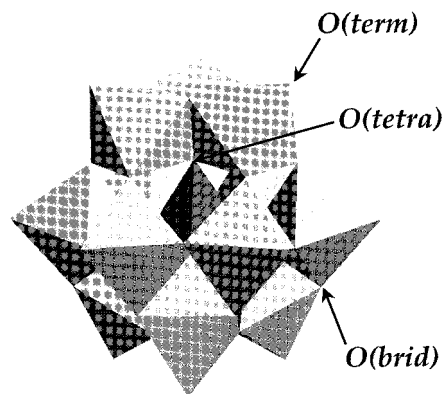
Contribution from the Departament de Química Física i Inorgànica and Institut d'Estudis Avançats, Universitat Rovira i Virgili, 43005 Tarragona, Spain, and Institut de Ciències de Materials de Barcelona, CSIC, Campus UAB, 08193 Bellaterra, Barcelona, Spain

Abstract: Calculations based on density functional theory (DFT) have been carried out to investigate the electronic and magnetic properties of the α-Keggin anions mentioned in the title. The atomic populations and the distribution of the electron density computed for the studied clusters support the hypothesis that an oxidized Keggin anion is an XO$_4$$^{n-}$ clathrate inside a neutral M$_{12}$O$_{36}$ cage. The energy gap between the band of occupied orbitals, formally delocalized over the oxo ligands, and the unoccupied d-metal orbitals, delocalized over the addenda, has been found to be independent of the central ion. However, substitution of a W or a Mo by V modifies the relative energy of the LUMO and then induces important changes in the redox properties of the cluster. In agreement with the most recent X-ray determination of [Co^{III}W$_{12}$O$_{40}$]$^{5-}$ and with the simplicity of the ^{183}W NMR and ^{17}O NMR spectra observed for this anion the calculations suggest that [Co^{III}W$_{12}$O$_{40}$]$^{5-}$ has a slightly distorted *T$_d$* geometry. For the parent cluster [CoW$_{12}$O$_{40}$]$^{6-}$ the quadruplet corresponding to the anion encapsulating a Co^{II} was found to be ∼1 eV more stable than the species formed by a Co^{III} and 1 e delocalized over the sphere of tungstens. The one-electron reduction of [Co^{II}W$_{12}$O$_{40}$]$^{6-}$ and [Fe^{III}W$_{12}$O$_{40}$]$^{5-}$ leads to the formation of the 1 e blue species [Co^{II}W$_{12}$O$_{40}$]$^{7-}$ and [Fe^{III}W$_{12}$O$_{40}$]$^{6-}$. The blue-iron cluster is considerably antiferromagnetic, and in full agreement with this behavior the low-spin state computed via a Broken Symmetry approach is 196 cm^{-1} lower than the high-spin solution. In contrast, the cobalt blue anion has a low ferromagnetic coupling with an S−T energy gap of +20 cm^{-1}. This blue species is more stable than the alternative reduction product [Co^{I}W$_{12}$O$_{40}$]$^{7-}$ by more than 0.7 eV.

Introduction

Heteropolyoxometalates (POMs) are those anions and their derivatives made of an assembly of MO$_6$ octahedrons. These octahedrons contain a central tetrahedron, XO$_4$, in which X is a main group element (P^V, Si^{IV}, Al^{III}, Ge^{IV}, etc.) or a transition metal ion (Fe^{III}, Co^{II}, Co^{III}, Cu^I, Cu^{II}, etc.).[1] The first POM, the phosphomolybdate [PMo$_{12}$O$_{40}$]$^{3-}$, was reported in 1826 by Berzelius,[2] and in 1864 Marignac observed two isomers, now designated by α and β, of the acid [H$_4$-SiW$_{12}$O$_{40}$].[3] The structure of the α-[PW$_{12}$O$_{40}$]$^{3-}$ was solved by Keggin (Figure 1) about 100 years after Berzelius' first report on POMs.[4] Today the series of compounds [XM$_{12}$O$_{40}$]$^{n-}$ are known as Keggin anions. In a recent review, Katsoulis described the large number and importance of the POM applications, which depend primarily on their redox properties, ionic charge, conductivity, etc.[5] Most of them are related to the special ability of the Keggin framework to accept electrons without decomposing. In reality, the Keggin core is a *reservoir* of electrons that can undergo many electron-reduction processes without significantly deforming the framework.[6]

Figure 1. Polyhedral representation of an α-Keggin structure.

Fully oxidized anions such as [PW$_{12}$O$_{40}$]$^{3-}$ or [SiW$_{12}$O$_{40}$]$^{4-}$, can undergo several rapid one- and two-electron reversible reductions to produce the so-called "heteropoly blue".[7] EPR spectra at different temperatures for the one-reduced species suggest that the spin can be partially localized at quite low temperatures but is delocalized at higher temperatures. This may mean that the spin is localized in the ground state but that it participates in a rapid thermal hopping from one metal to another

† Universitat Rovira i Virgili.
‡ Institut de Ciències de Materials de Barcelona.
(1) See for example: Pope, M. T. *Heteropoly and Isopoly Oxometalates*; Springer-Verlag: Berlin 1983; p 26.
(2) Berzelius, J. *Poggendorf's Ann. Phys.* **1826**, *6*, 369.
(3) Marignac, C. *Ann. Chim. Phys.* **1864**, *3*, 1.
(4) Keggin, J. F. *Nature* **1933**, *131*, 908.
(5) Katsoulis, D. E. *Chem. Rev.* **1998**, *98*, 359.

(6) Maestre, J. M.; Bo, C.; Poblet, J.-M.; Casañ-Pastor, N.; Gomez-Romero, P, *Inorg. Chem.* **1998**, *37*, 3444.
(7) See for exemple the review: Steckhan, E.; Sadakane, M. *Chem. Rev.* **1998**, *98*, 219 and references therein.

at higher temperatures.[8,9] The Keggin anion $[Co^{II}W_{12}O_{40}]^{6-}$ has particular interesting electronic properties since it can be reduced to obtain one $[Co^{II}W_{12}O_{40}]^{7-}$, or two $[Co^{II}W_{12}O_{40}]^{8-}$ electron-reduced derivatives, but $[Co^{II}W_{12}O_{40}]^{6-}$ can also be oxidized to give $[Co^{III}W_{12}O_{40}]^{5-}$. Indeed, this Co^{III} tungstate is a very strong oxidizing agent and has been referred to as a "soluble anode".[10] Another, interesting peculiarity of Keggin anions with a transition metal ion such as Fe^{III}, Co^{III}, or Co^{II} in the central position is the coexistence of several states and configurations in a relatively small energy range. Co^{II} occupies the cavity of the Keggin framework and retains the regular tetrahedral conformation. Therefore, the symmetry of the cluster is T_d like most of α-Keggin anions.[11] For the oxidized derivative $[Co^{III}W_{12}O_{40}]^{5-}$, a Jahn–Teller distortion has been reported for the Co$^{III}O_4$ tetrahedron.[12] However, a very simple NMR spectrum typical of an undistorted system has been observed for $[Co^{III}W_{12}O_{40}]^{5-}$.[13] Today, despite the abundant experimental data and considerable activity in the field of polyoxometales,[14] we believe that there is still a need for a systematic analysis of reduction effects on the molecular and electronic structure, reactivity, magnetism, physical properties, etc. of POMs.

In the past decade, Computational Transition Metal Chemistry has undergone an overwhelming change largely due to the widespread acceptance of density functional theory (DFT)-based methods.[15] The modeling of polyoxoanions is still incipient,[16] but it has been shown that it is suitable for the understanding of questions concerning the basicity of external oxygen sites,[17] the localization or delocalization of metal electrons in reduced species[6] and substituted ions,[18] and the identification of host and guest subunits in a cage complex.[19] Here, we report a detailed DFT study on the α-Keggin anions mentioned in the title with the aim of describing the electronic structure of these molecules and giving quantitative data about some of their properties.

Computational Details

Optimal geometries and their relative energies were computed by means of DFT formalism including gradient corrections for exchange and correlation. The formalism is based upon the local spin density approximation characterized by the electron gas exchange (Xα with $\alpha = 2/3$) together with Vosko–Wilk–Nusair[20] parametrization for correlation. Becke's nonlocal corrections to the exchange energy[21] and

Perdew's nonlocal corrections to the correlation energy[22] have been added. These calculations were carried out with the ADF program,[23] using triple-ζ + polarization Slater basis sets to describe the valence electrons of O, P, Si, and Al. For transition metal atoms, a frozen core composed of the 1s to 2sp shells for vanadium, cobalt, and iron; 1s to 3spd shells for molybdenum, and 1s to 4spdf for tungsten was described by means of single Slater functions. ns and np electrons were described by double-ζ Slater functions, nd and $(n+1)$s by triple-ζ functions and $(n+1)$p by a single orbital.[24–25] Quasi-relativistic corrections were used with the Pauli formalism and corrected core potentials. The quasi-relativistic frozen core shells were generated using the auxiliary program DIRAC.[23] Spin-unrestricted calculations were used to determine the energies of the high-spin states. The Broken Symmetry approach was used to compute the energies of the low-spin states involved in magnetic couplings. For some configurations we also report the multiplet energies calculated following the strategy proposed by Ziegler et al.[26] and developed later by Daul.[27] The idea is that in symmetric molecules with degenerate orbitals, the particular multiplets arising from an open-shell configuration, in general, cannot be expressed by a single determinant, and therefore, density functional calculations do not directly give multiplet energies. It is possible, however, to write the energy of a particular state as the weighted sum of single-determinant energies. This problem also arises in the calculations of states in Jahn–Teller (JT) distortions. To get consistent energies for the various points on the adiabatic potential surface associated with the JT distortions of $[Co^{III}W_{12}O_{40}]^{5-}$ we used the strategy suggested by Daul and co-workers.[28] Since the energy differences involved in JT distortions and magnetic couplings are very low, the value of the numerical integration parameter that we used to determine the precision of numerical integrals was 6.0, whereas for the other calculations it was 4.5.

All of the calculations reported here were carried out considering only the ions without the inclusion of the crystal environment. This approximation is reasonable for the purpose of the present study since in a previous study we showed that the crystal field is crucial for getting reasonable orbital energies, but the crystal environment does not necessarily modify either the ordering or the relative orbital energies of the cluster.[6] Therefore, the relative energies of the different states reported here should not be altered if isotropic fields are included. For systems that present short contacts between the anion and the counterions some of the conclusions reported here may not be able to be applied directly. A short-hand notation is used for the complexes, without oxygen atoms and anion charge, and it specifies the number of blue electrons as well as the substituted transition metal oxidation states (e.g., $[Co^{II}W_{12}O_{40}]^{6-} = Co^{II}W_{12}$ and $[Co^{II}W_{12}O_{40}]^{7-} = Co^{II}W_{12}$ 1e, where e specifies the number of blue electrons).

Results and Discussion

The Charge Localization in Keggin Anions: The Electronic Properties of the Fully Oxidized Anions $[P^VW_{12}O_{40}]^{3-}$, $[Si^{IV}W_{12}O_{40}]^{4-}$, and $[Al^{III}W_{12}O_{40}]^{5-}$. We will start by discuss-

(8) Baker, L. C.; Glick, D. C. *Chem. Rev.* **1998**, *98*, 3; Casañ-Pastor, N.; Bas-Serra, J.; Coronado, E.; Pourroy, G.; Baker, L. C. W. *J. Am. Chem. Soc.* **1992**, *114*, 10380.

(9) 25, 26, 88 NMR Sanchez, C.; Livage, J.; Launay, J. P.; Fournier, M.; Jeanin, Y. *J. Am. Chem. Soc.* **1982**, *104*, 3194; Sanchez, C.; Livage, J.; Launay, J. P.; Fournier, M *J. Am. Chem. Soc.* **1983**, *105*, 6817; Launay, J. P.; Fournier, M.; Sanchez, C.; Livage, J.; Pope, M. T. *Inorg. Nucl. Chem. Lett.* **1980**, *16*, 257.

(10) Eberson, L.; Wistrand, L.-G *Acta Chem. Scand. B* **1980**, *34*, 349; Walmsley, F. *J. Chem. Educ.* **1992**, *69*, 936.

(11) Casañ-Pastor, N.; Gomez-Romero, P.; Jameson, C. B.; Baker, L. C. W. *J. Am. Chem. Soc.* **1991**, *113*, 5658.

(12) Simmons, V. E. *Diss. Abstr. Int.* **1977**, *29b*, 926.

(13) Kazansky, L. P.; McGarvey, B. R. *Coord. Chem. Rev.* **1999**, *188*, 157 and references therein.

(14) Hill, C. L., Ed. *Chem. Rev.* **1998**, *98*, 1–390 (special issue on Polyoxometalates).

(15) Davidson, E. R, Ed. *Chem. Rev.* **2000**, *100*, 351–818 (special issue on Computational Transition Metal Chemistry).

(16) Rohmer, M.-M.; Benard, M.; Blaudeau, J.-P.; Maestre, J. M.; Poblet, J.-M. *Coord. Chem. Rev.* **1998**, *178–180*, 1019.

(17) (a) Kempf, J. Y.; Rohmer, M.-M.; Poblet, J.-M.; Bo, C.; Bénard, M. *J. Am. Chem. Soc.* **1992**, *114*, 1136; (b) Maestre, J. M.; Sarasa, J. P.; Bo, C.; Poblet, J.-M. *Inorg. Chem.* **1998**, *37*, 3071.

(18) Duclusaud, H.; Borshch, S. A. *Inorg. Chem.* **1999**, *38*, 3489.

(19) Rohmer, M.-M.; Benard, M. *J. Am. Chem. Soc.* **1994**, *116*, 6959; Rohmer, M.-M.; Devemy, J.; Wiest, R.; Benard, M. *J. Am. Chem. Soc.* **1996**, *118*, 13007.

(20) Vosko, S. H.; Wilk, L.; Nusair, M. *Can. J. Phys.* **1980**, *58*, 1200.

(21) Becke, A. D. *J. Chem. Phys.* **1986**, *84*, 4524; *Phys. Rev.* **1988**, *A38*, 3098.

(22) Perdew, J. P. *Phys. Rev.* **1986**, *B33*, 8882; **1986**, *B34*, 7406.

(23) *ADF 2.3 User's Guide*; Chemistry Department, Vrije Universiteit: Amsterdam, The Netherlnds, 1997; Baerends, E. J.; Ellis, D. E.; Ros, P. *Chem. Phys.* **1973**, *2*, 41; Fonseca Guerra, C.; Visser, O.; Snijders, J. G.; te Velde, G.; Baerends, E. J. *Methods and Techniques in Computational Chemistry: METECC-95*; Clementi, E., Corongiu, G., Eds.; STEF: Cagliari Italy, 1995; p 305.

(24) Snijders, J. G.; Baerends, E. J.; Vernooijs, P. *At. Nucl. Data Tables* **1982**, *26*, 483; Vernooijs, P.; Snijders, J. G.; Baerends, E. J. *Slater type basis functions for the whole periodic system*; Internal Report, Free University of Amsterdam: The Netherlands, 1981.

(25) Rosa, A.; Ricciardi, G.; Baerends, E. J.; Stufkens, D. J. *Inorg. Chem.* **1996**, *35*, 2886.

(26) Ziegler, T.; Rauk, A.; Baerends, J. E. *Theor. Chim. Acta* **1977**, *43*, 261.

(27) Daul, C. *Int. J. Quantum Chem.* **1994**, *52*, 867.

(28) Bruyndonckx, R.; Daul, C.; Manoharan, P. T.; Deiss, E. *Inorg. Chem.* **1997**, *36*, 4251.

Table 1. Comparison of DFT and X-ray[a] Distances (in Å) for a Series of α-Keggin Anions

		$[PW_{12}O_{40}]^{3-}$	$[SiW_{12}O_{40}]^{4-}$	$[AlW_{12}O_{40}]^{5-}$	$[Co^{III}W_{12}O_{40}]^{5-}$	$[Co^{II}W_{12}O_{40}]^{6-}$	$[Co^{II}W_{12}O_{40}]^{7-}$	$[Fe^{III}W_{12}O_{40}]^{5-}$
$X-O_{tetra}$	DFT	1.574	1.667	1.796	1.821	1.896	1.897	1.823
	expt	1.53	1.64	1.74	1.79	1.90		1.82
$W-O_{tetra}$	DFT	2.424	2.325	2.242	2.265	2.203	2.215	2.263
	expt	2.43	2.35	2.26		2.16		
$X-W$	DFT	3.579	3.532	3.526	3.565	3.547	3.559	3.567
	expt	3.49		3.51		3.49		3.53
$W-O_{ter}$	DFT	1.727	1.743	1.763	1.771	1.784	1.797	1.773
	expt	1.69	1.71	1.71	1.71	1.71		1.72
$W-O_{brid}$	DFT	1.932	1.916	1.930	1.943	1.946	1.951	1.944
		1.936	1.937	1.955	1.968	1.978	1.982	1.968
	expt[b]	1.90−1.91		1.90−1.96	1.85−1.97	1.88−1.99		1.88−1.96
ref (expt)		57	58	29	37	11		36

[a] Averaged values/ [b] Observed interval values are given for the $W-O_{brid}$ bond.

Table 2. Net Charges Computed for Several α-Keggin Anions: Notice the Strong Relationship between the Total Charge of the Anion and the Charge Localized on the Internal Tetrahedron XO_4

	$[PW_{12}O_{40}]^{3-}$	$[SiW_{12}O_{40}]^{4-}$	$[AlW_{12}O_{40}]^{5-}$	$[Fe^{III}W_{12}O_{40}]^{5-}$	$[Co^{III}W_{12}O_{40}]^{5-}$	$[Co^{II}W_{12}O_{40}]^{6-}$	$[Co^{II}W_{12}O_{40}]^{7-}$
XO_4							
total charge	−1.66	−2.59	−3.09	−4.03	−3.98	−4.47	−4.42
relative charge[a]	0	−0.93	−1.4	−2.4	−2.3	−2.8	−2.8
O_{ter} [b]	−0.78	−0.82	−0.89	−0.85	−0.85	−0.89	−0.92
O_{brid} [b]	−1.06	−1.05	−1.05	−1.02	−1.02	−1.02	−1.02
	−1.12	−1.12	−1.09	−1.07	−1.07	−1.07	−1.06
W^b	+2.85	+2.87	+2.85	+2.86	+2.85	+2.85	+2.79

[a] Relative charge of XO_4 subunits taken as zero the net charge of the less charged anion, $[PW_{12}O_{40}]^{3-}$. [b] Mulliken charges for O_{ter}, O_{brid}, and W in the isolated neutral cage $W_{12}O_{36}$ with its structure in the anion $[PW_{12}O_{40}]^{3-}$ are −0.64, −1.05, and +2.76 e, respectively.

ing those Keggin anions whose heteroatom is a main group element. The structures of the isoelectronic PW_{12}, SiW_{12}, and AlW_{12} clusters were optimized under the restrictions of the T_d symmetry group. The metal−oxygen bonds in an α-Keggin framework can be divided into three sets according to whether their oxygen atoms is tetrahedral (tetra), bonding (bond), and terminal (ter) (Figure 1). In addition, there is a fourth metal−oxygen bond between the heteroatom and O_{tetra}. In all of the structures, the computed geometries agree very well with the experimental ones, and the major discrepancies appears in the $W-O_{ter}$ and $X-O_{tetra}$ bonds, which are underestimated by an average of ∼0.04 Å (See Table 1). In a recent study on α and β Keggin anions, Weinstock et al.[29] showed that the $X-O_{tetra}$ bond lengths change with X. However, the size of the cavity occupied by the XO_4 group into the $W_{12}O_{36}$ framework remains fairly constant. They reported that the sum of X−O and W−O bond lengths is 4.00, 3.97, and 3.96 Å for X = Al, Si, and P, respectively. This similarity was believed to support the hypothesis that Keggin anions are anionic XO_4 units encapsulated by the neutral $W_{12}O_{36}$ cages.[30] Clark and Hall[31] also suggested that PMo_{12} is a clathrate structure in which the PO_4^{3-} subunit is trapped into the $Mo_{12}O_{36}$ cage. Jansen et al. from Extended Hückel calculations already suggested such a localization.[32] Present calculations perfectly reproduce this trend since for the silico- and phosphotungstate anions the sum of X−O and W−O bond lengths were computed to be 3.99 Å, and when the central position is occupied by a Al^{III}, that sum increases slightly (∼0.04 Å). The Mulliken atomic charges given in Table 2 evidence that there is a close relationship between the *total charge* of the anion and the *charge associated with the XO₄ unit* in agreement with Day and Klemperer's hypothesis of charge localization.[30] It is well-known that the Mulliken charges

in some cases have little meaning, but in general the charge differences are much more believable. For PW_{12}, the Mulliken analysis assigns an electronic charge of −1.66 e to XO_4. This negative charge increases by 0.93 e for SiW_{12}, and by 1.4 e for AlW_{12}. Although the electronic structure of the Keggin anions with paramagnetic heteroatoms will be discussed in detail in the next section, it is of interest here to mention the computed charges found for the ground states of $[Co^{III}W_{12}O_{40}]^{5-}$ and of its reduced species $[Co^{II}W_{12}O_{40}]^{6-}$. The net charges supported by the CoO_4 tetrahedron in these two cobalt complexes is −3.98 and −4.47 e. These values are 2.3 and 2.8 e in excess of the charge on the PO_4 tetrahedron in $[PW_{12}O_{40}]^{3-}$. The net charge of −4.42 e associated with the internal tetrahedron in $[Co^{II}W_{12}O_{40}]^{7-}$ is also consistent with the rest of the series, since the additional electron in the reduced cluster goes to the outer sphere of tungstens and not to the internal tetrahedron. This subject will be discussed below in depth. In summary, we can conclude that a fully oxidized Keggin anion $[XM_{12}O_{40}]^{n-}$ may be described as a neutral $M_{12}O_{36}$ cage that encapsulates a XO_4 anion and that it can also be formulated as $[XO_4^{n-}@M_{12}O_{36}]$.

The concentration of the global charge in the XO_4 unit induces a strong polarization of the electron distribution of the almost neutral $M_{12}O_{36}$ cage. The map in Figure 2 displays the deformation density distribution $\Delta\rho$,[33] computed for the phosphotungstate anion as

$$\Delta\rho = \rho_{Keggin} - (\rho_{XO_4^{n-}} + \rho_{M_{12}O_{36}})$$

In this map, the solid lines are positive contours and represent regions of charge accumulation, while dotted lines are negative contours and represent regions of charge depletion. The encapsulation of the tetrahedral ion by the $W_{12}O_{36}$ cage polarizes the two fragments and thus increases their mutual electrostatic interaction. In accordance with this behavior, accumulations

(29) Weinstock, I. A.; Cowan, J. J.; Barbuzi, E. M. G.; Zeng, H.; Hill, C. L. *J. Am. Chem. Soc.* **1999**, *121*, 4608.
(30) Day, V. W.; Klemperer, W. G. *Science* **1985**, *228*, 533.
(31) Clark, C. J.; Hall, D. *Acta Crystallogr.* **1976**, *B32*, 1454.
(32) Jansen, S. A.; Singh, D. J.; Wang, S.-H. *Chem. Mater.* **1994**, *6*, 146.

(33) Schwarz, W. H. E.; Ruedenberg, K.; Mensching, L. *J. Am. Chem. Soc.* **1989**, *111*, 6926; *Electron Distributions and the Chemical Bond*; Coppens, P., Hall, M. B., Eds.; Plenum: New York, 1982.

Figure 2. Deformation density map for $[PW_{12}O_{40}]^{3-}$ computed as a difference between the density of the molecule minus the density sum of the two fragments, PO_4^{3-} and $W_{12}O_{36}$. The density is represented in a plane containing the heteroatom, two oxygens belonging to the inner tetrahedron, and two tungsten atoms and their associated terminal oxygens and four bridging oxygens.

associated to the XO_4 fragment are consistently oriented toward the W atoms, whereas the entire region around the phosphorus nucleus is a zone of charge depletion. The polarization in the tungstate fragment is simply opposite to the polarization of XO_4. Tungsten atoms already have an oxidation state of $+VI$ in $W_{12}O_{36}$, and this is shown by an important positive charge of $+2.76$ e in the isolated cage. These atoms increase slightly their depopulation when a Keggin cluster forms. The computed charge for W's is $+2.85$ e in the PW_{12} anion. Together with this depopulation of the metal atoms there are strong accumulations of charge density in the outer sphere of the POM, specially concentrated in the terminal oxygens. A direct consequence of the polarization of $W_{12}O_{36}$ is that the presence of an ion inside the cage increases the *basicity of the external oxygens* and that this increase correlates with the *net charge of the anion*. In previous studies, we showed that there is a relationship between the basicity of the external oxygens and the number and type of metals connected to the oxygen site.[17]

For Keggin anions without paramagnetic ions the ground-state configuration is typical of a fully oxidized polyoxoanion with a large energy gap between the HOMO, formally delocalized over oxo-ligands, and the LUMO, delocalized over the d-shells of tungstens. The energy gap between the occupied and unoccupied band in fully oxidized Keggin anions is almost independent of the nature of X. For tungstates, this energy difference was computed to be ~2.8 eV (Figure 3). This value decreases by up to 2 eV for molybdates. Indeed, the lower d-metal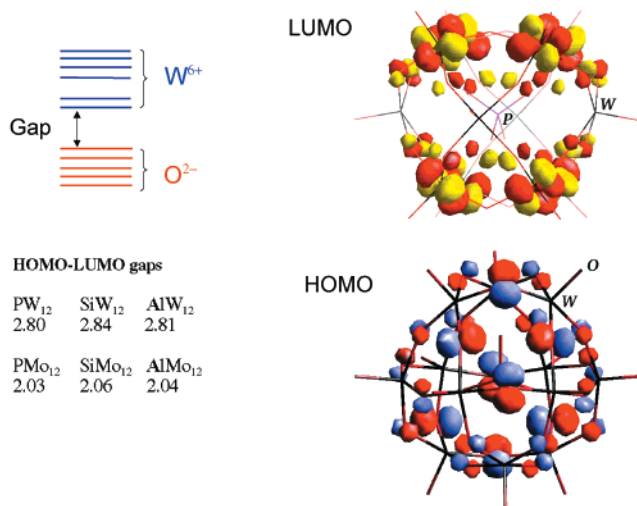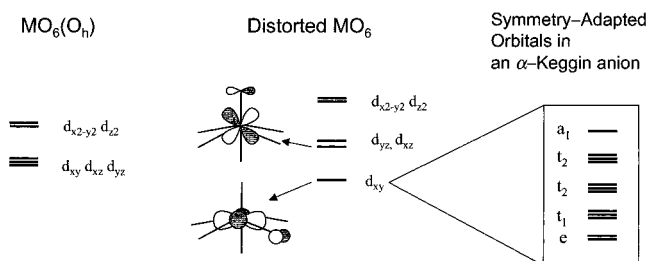 orbitals in molybdates mean that they can be more easily reduced to give heteropoly blues. Hence, for instance, $SiMo_{12}$ and $GeMo_{12}$ are more powerful oxidizing agents than the corresponding tungstates by ~0.5 V.[34]

The unoccupied orbitals of fully oxidized Keggin anions are symmetry-adapted d-metal orbitals with some antibonding participation of oxygen orbitals (Scheme 1). The metals in the $M_{12}O_{36}$ framework are in an octahedral environment, but since the MO_6 units do not retain a perfect octahedral symmetry, the e_g and t_{2g} orbitals are not degenerated. Because of the high oxidation state of metals in POMs the t_{2g} like orbitals are the most interesting in these clusters. Indeed, d_{xy}, d_{xz}, and d_{yz} orbitals are destabilized by antibonding interactions with appropriate

Figure 3. Schematic orbital diagram, HOMO−LUMO energy gaps (in eV) and 3D representations of one of the two doubly degenerate components of the LUMO and HOMO, the fully oxidized $[PW_{12}O_{40}]^{3-}$ anion. The contribution of oxo-ligand orbitals to the LUMO is ~95%, and for the HOMO the highest weight is for d−W orbitals with a contribution of 73%.

Scheme 1

symmetry p oxygen orbitals. The negative overlap is notably higher for terminal than for bridging oxygens because the metal−oxygen bond lengths are shorter and the orientations are more favorable. As a matter of fact, the lowest metal orbitals in these anions are symmetry-adapted combinations of d_{xy}-like orbitals, the lowest one being an orbital of symmetry e, for which a 3D representation is given in Figure 3. As Scheme 1 shows, the LUMO + 1 is a triply degenerate orbital of symmetry t_1. Two sets of orbitals of symmetry t_2 and one of symmetry a_1 fulfill the $12T_d$ symmetry-adapted combinations of the d_{xy}-like orbitals of the $M_{12}O_{36}$ framework. The next orbitals are a series that are symmetry-adapted combinations of the d_{xz}- or d_{yz}-like orbitals.

Heteropoly Complexes Containing Paramagnetic Ions: The Ground States for $[Co^{III}W_{12}O_{40}]^{5-}$, $[Co^{II}W_{12}O_{40}]^{6-}$, and $[Fe^{III}W_{12}O_{40}]^{5-}$. For a d^6 ion in a tetrahedral environment two configurations can have similar energies: the low-spin configuration with $S = 1$ and the high-spin configuration with $S = 2$ (Scheme 2). The structure of $[Co^{III}W_{12}O_{40}]^{5-}$ has one controversial point. Yanonni's first X-ray characterization showed that the $Co^{III}O_4$ tetrahedron is elongated: it has three pairs of oxygen−oxygen distances of 2.69, 3.20, and 3.31 Å.[35] In contrast, the anions $[Co^{II}W_{12}O_{40}]^{6-}$[11] and $[Fe^{III}W_{12}O_{40}]^{5-}$[36] present undistorted tetrahedral frameworks. Subsequently, Simmons[12] proposed two distinct oxygen−oxygen distances of 2.7 and 3.5 Å for O_{tetra}−O_{tetra} separations in the Co^{III} species. On

(34) Sedane, M.; Steckhan, E. *Chem. Rev.* **1998**, *98*, 219; Altenan, J. J.; Pope, M. T.; Prados, R. A.; So, H. *Inorg. Chem.* **1975**, *14*, 417; Maeda, K.; Katano, H.; Osakai, T.; Himeno, S. *Electroanal. Chem.* **1995**, *389*, 167.

(35) Yannoni, N. F. Ph.D. Thesis, Boston University, 1961.
(36) Le Magueres, P.; Oualab, L.; Golhen, S.; Grandjean D.; Peña, O.; Jegaden, J.-C.; Gomez-Garcia, C. J.; Delhaes, P. *Inorg. Chem.* **1994**, *33*, 5180.

the basis of these structural data a Jahn−Teller distortion was proposed for this oxidized species as Kazansky and Garvey explain at length in a recent review on the NMR properties of polyoxoanions.[13] More recently, Muncaster et al.[37] reported a new characterization of $K_5[CoW_{12}O_{40}]$ for which the authors found that the cobalt is in a slightly distorted tetrahedral environment with an average Co−O bond distance of ~1.79 Å and the O_{tetra}−O_{tetra} distances ranging from 2.87 to 2.96 Å.

Scheme 2

$$S=1 \ (+0.51\text{eV}) \qquad S=2 \ (0.0)$$

The first calculations were made for the high- and low-spin configurations under the T_d group restrictions. In full agreement with all of the experimental determinations, which identify $Co^{III}W_{12}$ as a high-spin complex,[38] the electronic configuration with $S = 2$ was computed to be more stable than the configuration with four electrons in the orbital of symmetry e, but the energy difference between the two configurations may be considered relatively small, 0.51 eV. The bond distances obtained for the optimal geometry (Table 1) of this cobalt− tungstate anion compare well with the most recent experimental values derived from X-ray data and reported by Muncaster et al. As for the diamagnetic systems XW_{12}, with X = P, Si, and Al the major deviation between the optimized and the observed bond distances is in the W−O_{term} bond length (~0.06 Å). No significant differences were observed between the two optimal geometries for the high- and low-spin complexes. Figure 4a shows the energies and symmetries of some frontier orbitals computed at the unrestricted level for the optimal geometry of $Co^{III}W_{12}$ in the ground configuration $e^3 t_2^3$. There are two important points in Figure 4a. On one hand, the three sets of orbitals, the doubly occupied orbitals delocalized over O^{2-} ligands, the d-cobalt orbitals, and the vacant orbitals delocalized over tungstens are very well separated in composition and energy with the exception of the unoccupied cobalt β orbital $33t_2$ which is near the tungsten band. Another important peculiarity is that the substitution of a main group element by a transition metal does not change the energy gap between the doubly occupied oxygen orbitals and the unoccupied metal orbitals. The value of 2.7 eV is similar to the HOMO−LUMO gap computed for the main group element clusters XW_{12}, X = Al, Si, and P (~2.8 eV).

The partial occupation of the doubly degenerate orbital in the lowest configuration allows a Jahn−Teller distortion of $Co^{III}W_{12}$. Since in the D_{2d} symmetry the orbital of the e symmetry splits into a_1 and b_1 there are two different ways of accommodating three electrons, $a_1^2 b_1^1$ and $a_1^1 b_1^2$ (Scheme 3). The result of optimizing these two configurations under the restrictions of the D_{2d} group were two structures: a slightly *flattened* and a slightly *elongated* tetrahedron with associated stabilizations of 470 and 440 cm^{-1}, respectively. In both cases, the geometric changes are quite small: the deviations from the regular tetrahedral angle do not exceed 3°, and the variations in the Co−O_{tetra} bond length are −0.004 Å in both the flattened and elongated forms. These slight distortions and low energies seem to be in agreement with the most recent X-ray determi-

(37) Muncaster, G.; Sankar, G.; Catlow, C. R. A.; Thomas, J. M.; Coles, S. J.; Hursthouse, M. *Chem. Mater.* **2000**, *12*, 18.
(38) Acerete, R.; Casañ-Pastor, N.; Bas-Serra, J.; Baker, L. C. W. *J. Am. Chem. Soc.* **1989**, *111*, 6049.

nation of $K_5[CoW_{12}O_{40}]$ [37] and with the fact that this ion gives a single line in the ^{183}W NMR spectrum and three lines in the ^{17}O NMR spectrum. The simplicity of these spectra[38−39] may be associated with a dynamic Jahn−Teller distortion in solution that would average the tungsten resonances and give rise to only three oxygen resonances. The $S = 1$ case is also JT active. The $a_1^2 b_1^2 e^2 b_2^0$ is the lowest configuration in the D_{2d} symmetry and has a JT stabilization of 750 cm^{-1}.

Scheme 3

$$0.0 \qquad -470\text{cm}^{-1} \qquad -440 \text{ cm}^{-1}$$

It is well established that the one-electron reduction of $Co^{III}W_{12}$ yields $Co^{II}W_{12}$ and not the blue species $Co^{III}W_{12}1e$.[38] In the reduced system, the ground state is a quadruplet with three unpaired electrons in orbital $33t_2$. The Co−O_{tetra} bond length increases from 1.821 Å in the Co^{III} complex to 1.896 Å in the reduced system, which corroborates that the extra electron is localized in the internal tetrahedron. This lengthening may be because of an increase in the Pauli repulsion between the oxo-ligands and cobalt electrons. A similar variation but of opposite sign takes place for the O_{tetra}−W bond length. We have already mentioned that the X−W separation is almost invariant with X. Thus, any lengthening in the X−O_{tetra} bond length automatically shortens the vicinal O_{tetra}−W bond (Table 1). The most important difference between the orbital diagrams for Co^{III} and Co^{II} species (Figure 4a and 4b) is that in the reduced cluster orbital $33t_2$ of β nature inserts into the tungsten band. The high energy of this orbital is the reason there is no $Co^{I}W_{12}$ in the one-electron reduction of $Co^{II}W_{12}$ since the fundamental product is the blue species $Co^{II}W_{12}$ 1e. Table 3 shows the spin density values ($\alpha-\beta$ electrons) computed for several clusters using the Mulliken procedure. In $Co^{II}W_{12}$, these values are dominated by the three unpaired spins of the t_2 orbitals, which are strongly localized on the cobalt center (+2.56 e) but have a small contribution over the tetrahedral oxygens (+0.066 e per center). If one electron is removed from orbital $18e$ to give rise to the oxidized Co^{III} species, there is an increase in the spin density in the heteroatom (+0.3 e) but the major change occurs in the tetrahedral oxygens (+0.64 e if the four atoms are considered).

To check the energies computed for open-shell configurations, which at the unrestricted level represent an average of the individual multiplet energies associated with a given configu- ration, we also determined the energies of the highest-spin multiplets arising from configurations $e^4 t_2^2$ ($^3T_1$) and $e^3 t_2^3$ (^5E) in $Co^{III}W_{12}$ and from configurations $e^4 t_2^3$ ($^4A_2$) and $e^3 t_2^4$ ($^4T_2$) in $Co^{II}W_{12}$. The multiplet energies were computed with the aid of the STAGEN program for determining the symmetry coefficients for wave functions and energies. Daul described the method in detail and illustrated it with several simple examples.[27] Using this procedure the energy of the $^3T_1$ associ- ated with the excited configuration $e^4 t_2^2$ was found to be higher than the ground state ^5E by 0.30 eV, and the relative energy between the $^4T_2$ and $^4A_2$ in the reduced species was 0.88 eV. Schemes 2 and 4 show in both cases the average multiplet energies derived from monodeterminantal calculations, which

(39) Kazanskii, L. P.; Fedotov, M. A. *Koord. Khim.* **1988**, *14*, 939.

a

$$\left[Co^{III}W_{12}O_{40}\right]^{5-}$$

b

$$\left[Co^{II}W_{12}O_{40}\right]^{6-}$$

c

$$\left[Fe^{III}W_{12}O_{40}\right]^{5-}$$

Figure 4. Symmetries and energies (in eV) of some frontier orbitals computed at the unrestricted level for several heteropolyanions with paramagnetic ions for $[Co^{III}W_{12}O_{40}]^{5-}$ (a), $[Co^{II}W_{12}O_{40}]^{6-}$ (b), and $[Fe^{III}W_{12}O_{40}]^{5-}$ (c).

are reasonably good approximations of the multiplet energies since the differences between both procedures do not exceed 0.2 eV. Using Daul's strategy we are now carrying out a systematic study of several configurations and states for $[Co^{II}Cl_4]^{2-}$ and $[Co^{II}W_{12}O_{40}]^{6-}$ to reproduce and interpret the electronic spectra of these anions. This work will be published elsewhere.[40]

Configurations corresponding to a Co^{III} and one blue electron were also studied (Scheme 4). The lowest one, which had a relative energy with respect to the ground configuration of 0.98 eV, corresponds to the promotion of one electron from orbital 18e localized on Co to orbital 19e formally delocalized over the tungstens. The relative energy of the alternative configuration $18e^4 \, 33t_2{}^2 \, 19e^1$ is 1.39 eV. Excitations to higher W-orbitals were

(40) Maestre, J. M.; Lopez, X.; Bo, C.; Daul, C, Poblet, J.-M. to be published.

Table 3. Spin Densities ($\alpha-\beta$) Computed for Several Structures

	$Co^{III}W_{12}$	$Co^{II}W_{12}$	$Co^{II}W_{12} 1 \, e \, (HS)$	$Co^{II}W_{12} 1 \, e(LS)$
Co	+2.867	+2.565	+2.573	+2.578
W	−0.003	+0.002	+0.088	−0.083
O_{tetra}	+0.226	+0.066	+0.063	+0.066
O_{ter}	+0.006	+0.002	−0.004	+0.008
O_{brid}	+0.002	+0.001	+0.003	−0.001
	+0.015	+0.008	+0.011	+0.005

	$Fe^{III}W_{12}$	$Fe^{III}W_{12} 1 \, e \, (HS)$	$Fe^{III}W_{12} 1 \, e(LS)$
Fe	+4.003	+4.018	+3.908
W	−0.001	+0.084	−0.054
O_{tetra}	+0.193	+0.189	+0.133
O_{ter}	+0.006	0.000	+0.008
O_{brid}	+0.002	+0.004	+0.000
	+0.012	+0.015	+0.009

Scheme 4

Scheme 5

always computed at higher energies. These significant energies explain why $Co^{III}W_{12}1e$ was not the reduction product of $Co^{III}W_{12}$. It is worth noting that, although in some cases we refer to the band of unoccupied orbitals, this set of orbitals does not conform an energy band in the strict sense since the different molecular orbitals are separated by relative important energies. Consequently, discrete excitation energies result from Co → W transitions. For example, the electronic transition $33t_2 → 22t_1$ appears displaced with respect to $33t_2 → 19e$ transition in 0.33 eV (see Figure 4b for the numeration of the orbitals). In larger systems, such as $[V_{34}O_{82}]^{10-}$, molecular orbitals are structured in bands, and the presence of metal electrons leads to species with large numbers of unpaired electrons.[41]

In contrast to cobalt−tungstate anions the highest occupied orbitals in $[Fe^{III}W_{12}O_{40}]^{5-}$ are less pure d-orbitals, that is, the d-iron orbitals occupied in the high-spin configuration are mixed with the valence orbitals of the inner oxygens. Despite this mixing, the computed ground state for $Fe^{III}W_{12}$ corresponds to the configuration with spin $5/2$ as the spin density population of Table 3 shows. Four of the five α electrons are localized on the iron center, and the rest of the spin density is delocalized over the four tetrahedral oxygens (0.19 e per oxygen). It is also interesting to note that in the iron complex the $β$ unoccupied d-orbitals are quite high in energy. Hence, the e symmetry orbitals are separated from the tungsten band by only 0.19 eV, the corresponding energy gap in the Co^{II} complex being 0.58 eV (Figure 4b and 4c). This small separation between tungsten and iron orbitals is important since it does not allow the iron ion to be reduced from Fe^{III} to Fe^{II}. All attempts to get the $e^3 t_{2g}^3$ configuration were unsuccessful since the additional electron was always transferred from the iron to the tungsten set of orbitals. These results agree with the observed reactivity since one- or two-electron reduction of $Fe^{III}W_{12}$ yielded the blue species.[42] If we compare the net charge distribution (Table 2) inside the two anions $Fe^{III}W_{12}$ and $Co^{III}W_{12}$, both of which have the same total negative charge, we observe that there is no noticeable difference. Again this shows that the total charge on the XO_4 fragment is the key element in the charge distribution of the cluster. The unperceptible changes in the geometry also show that the geometry of the cluster is also dominated by the total charge on the tetrahedral fragment (Table 1).

The Blue Electron Species with Paramagnetic Ions: Magnetic Couplings between Blue Electrons and Paramagnetic Ions. One of the most active research fields in polyoxometalates in the past decade has been the preparation and the understanding of magnetic complexes.[43,44] In particular, the magnetic interactions between delocalized blue electrons and paramagnetic centers have been the object of study by several techniques, namely magnetic measurement on solids down to liquid helium, Evans susceptibility methods made with reference to the oxidized forms, and ^{183}W NMR in solution.[43a,45,46] While no interaction or an antiferromagnetic interaction has been observed when one paramagnetic ion is present, two-electron reductions induce notable magnetic changes that are not logical

if both blue electrons are strongly antiferromagnetically coupled. Delocalization of the spin density of the blue electron pair is sure to occur within the octahedral sites and to a lesser extent on the tetrahedral site.

From the theoretical point of view progress has been made in the quantitative determination of coupling exchange constants by means of multideterminantal approaches.[47,48] These methodologies give very accurate estimates of the coupling constants, but they are very computationally demanding and are presently limited to medium-sized molecules. The Broken Symmetry (BS) approach proposed by Noodleman et al.[49] has been shown to be an acceptable alternative that can be applied to larger systems.[50] We used this strategy to compute LS states complementary to the lowest HS configurations corresponding to $Fe^{III}W_{12}$ 1e and $Co^{II}W_{12}$ 1e (Scheme 5). When an α blue electron is aggregated to the $Fe^{III}W_{12}$ framework, the variations in the spin density are located on the sphere of tungstens, and each metal center contains the fractional part of 1 e (0.084 α electron per center). As Table 3 shows, the one-electron reduction of the iron cluster causes no significant alteration in the electronic distribution inside the $Fe^{III}O_4$ tetrahedron. Neither the total net charges nor the spin densities are changed by the
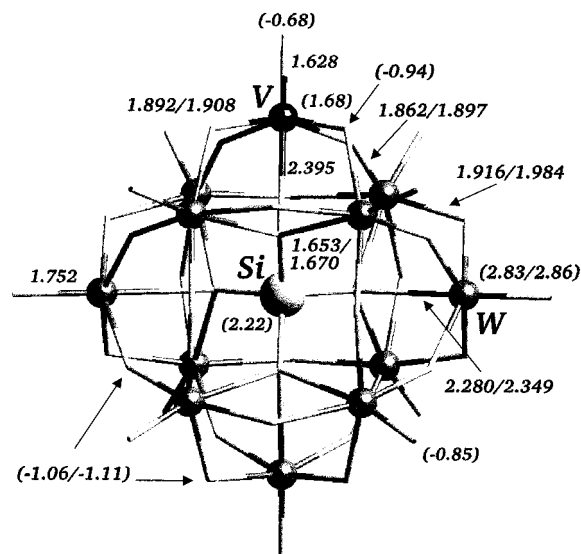
(41) Poblet, J.-M.; Bénard, M. unpublished results.

(42) Varga, G. M. Doctoral Dissertation, Georgetown University, 1968; *Diss. Abs. Int.* **1971**, *29B*, 926.

(43) (a) Casañ-Pastor, N.; Baker, L. C. W. In *Polyoxometalates*, Pope, M. T. M., Müller A., Eds.; Kluwer: The Netherlands, 1994, 203. (b) Casañ-Pastor, N.; Bas-Serra, J.; Coronado, E. Pourroy, G.; Baker, L. C. W. *J. Am. Chem. Soc.* **1992**, *114*, 10380. (c) Muller, A.; Peters, F.; Pope, M. T.; Gatteschi, D. *Chem. Rev.* **1998**, *98*, 239. (d) Gatteschi, D.; Sessoli, R.; Plass, W.; Muller, A.; Krickemeyer, E.; Meyer, J.; Sölter, D.; Adler, P. *Adv. Inorg. Chem.* **1996**, *35*, 1926.

(44) Coronado, E.; Galán-Mascarós, J. R.; Giménez-Saiz, C.; Gómez-García, C. J.; Triki, S. *J. Am. Chem. Soc.* **1998**, *120*, 4671; Clemente-Juan, J. M.; Coronado, E. *Coord. Chem. Rev.* **1999**, *193−195*, 361; Clemente-Juan, J. M.; Andres, H.; Borrás-Almenar, J. J.; Coronado, E.; Güdel, H. U.; Aebersold, M.; Kearly, G.; Büttner, H.; Zolliker, M. *J. Am. Chem. Soc.* **1999**, *121*, 10021; Andres, H.; Clemente-Juan, J. M.; Aebersold, M.; Güdel, H. U.; Coronado, E.; Büttner, H.; Kearly, G.; Melero, J.; Burriel, R. *J. Am. Chem. Soc.* **1999**, *121*, 10028.

(45) Kozik, M.; Casañ-Pastor, N.; Hammer, C. F.; Baker, L. C. W. *J. Am. Chem. Soc.* **1988**, *110*, 7697.

(46) Casañ-Pastor, N.; Baker, L. C. W. *J. Am. Chem. Soc.* **1992**, *114*, 10384.

(47) Castell, O.; Miralles, J.; Caballol, R. *Chem. Phys.* **1986**, *85*, 1427; Castell, O.; Caballol, R.; García, V.; Handrick, K. *Inorg. Chem.* **1996**, *35*, 1609.

(48) De Loth, P.; Cassoux, P.; Daudey, J. P.; Malrieu, J. P. *J. Am. Chem. Soc.* **1981**, *103*, 4007; Charlot, M. F.; Verdaguer, M.; Journaux, Y.; de Loth, P.; Daudey, J. P. *Inorg. Chem.* **1984**, *23*, 3802; Wang, C.; Fink, K. Staemmler, V. *Chem. Phys.* **1994**, *201*, 87; Fink, K. Staemmler, V *Inorg. Chem.* **1994**, *33*, 6219; Erasmus, C.; Haase, W. *Spectrochim Acta* **1994**, *50A*, 2189.

(49) Noodleman, L. *J. Chem. Phys.* **1981**, *74*, 5737; Noodleman, L.; Davidson, E. R. *Chem. Phys.* **1986**, *109*, 131; Noodleman, L.; Case D. A. *Adv. Inorg. Chem.* **1992**, *31*, 423; Noodleman, L.; Peng, C. Y.; Case D. A. *J. Coord. Chem. Rev.* **1995**, *144*, 199.

(50) Ruiz, E.; Cano, J.; Alvarez, S.; Alemany, P. *J. Comput. Chem.* **1999**, *20*, 1391; Ruiz, E.; Alemany, P.; Alvarez, S.; Cano, J. *J. Am. Chem. Soc.* **1997**, *119*, 1297; Ruiz, E.; Alemany, P.; Alvarez, S.; Cano, J. *Inorg. Chem.* **1997**, *36*, 3683; Ruiz, E.; Alemany, P.; Alvarez, S. *Chem. Commun.* **1998**, 2767; Cano, J.; Ruiz, E.; Alemany, P.; Lloret, F.; Alvarez, S. *J. Chem. Soc., Dalton Trans.* **1999**, 1669; Cano, J.; Alemany, P.; Alvarez, S.; Verdaguer, M.; Ruiz, E. *Chem. Eur. J.* **1998**, *4*, 476; Ruiz, E.; Cano, J.; Alvarez, S.; Alemany, P. *J. Am. Chem. Soc.* **1998**, *120*, 11122.

presence of the blue electron in the addenda. In the LS state the extra beta electron can go to orbital 18 e that mainly consist of d-iron orbitals or to orbital 19e, which is basically a symmetry-adapted d_{xy} W-orbital. Only 0.2 eV separates these two orbitals in the oxidized partner. We have already mentioned that we could not get the Kohn–Sham solution for the reduced species $Fe^{II}W_{12}$ since the SCF process yielded the LS state with a β blue electron. In contrast to the ferromagnetic state the antiferromagnetic coupling is characterized by a certain transfer of charge density, especially of β type, from the addenda to the internal tetrahedron. Hence, the population of the iron ion increased by 0.09 e of β type after the reduction of the cluster and although it is true that the total population of the tetrahedral oxygens does not change, their spin density decrease from 0.19 e in the oxidized species to 0.13 e in the reduced cluster. Taking the fragment as a whole, the total negative charge increases slightly from −4.027 to −4.200 e after reduction, whereas the spin density decreases from 4.78 to 4.44 e. This is the result of mixing 18e and 19e orbitals, and it slightly delocalizes the blue electron into the internal tetrahedron. In full agreement with the *antiferromagnetic* behavior[46] observed for the blue species $Fe^{III}W_{12}$ 1 e, the low-spin configuration with five α electrons localized on Fe and a β electron formally delocalized among tungstens was found to be more stable than the state characterized by six α electrons. The energy difference between the HS and LS states was computed to be 196 cm^{-1}.

At this point it must be pointed out that the BS states are not *physical* states. When they are projected onto $\hat{S}^2$ eigenfunctions, the energy difference, in general, increases. This energy difference may depend on the functional used and on the delocalization it induces. However, the BS+DFT formalism correctly gives the sign of the coupling constants. Thus, the magnetic energies reported here must be taken as approximate values for the energy gap between the actual high- and low-spin states that in this case are a heptuplet and a quintuplet. For further discussion about this problematic, see Caballol, Illas et al.[51] and the recent review of Illas et al.[52] For the cobalt anion the energy difference between the high- and low-spin states (Scheme 5) was found to be extremely low (20 cm^{-1}), and the *ferromagnetic* state in this case is the lowest. $Co^{II}W_{12}$ 1 e species can be prepared in solution, stoichiometrically, and their properties measured by Evans ^{1}H NMR method, at room temperature, using $Co^{II}W_{12}$ as reference. This measurement shows a magnetic moment for the 1 e blue anion corresponding to no interaction between the Co^{II} center and the delocalized blue electron, at room temperature. However, the 1 e blue cannot be isolated in solid form, since it always disproportionates into $Co^{II}W_{12}$ 2e (in solid form) and $Co^{II}W_{12}$, for whatever cation tried, in slow crystallizations with K$^+$ or fast precipitations with guanidium salts. Therefore, the low-temperature magnetic properties, which could show the existence of any interaction, have never been possible. ^{183}NMR for $Co^{II}W_{12}$ 1 e has not been possible to obtain either due to fast relaxation related with the delocalized electron.

Magnetic couplings between the blue electron and Co^{II} in $Co^{II}W_{12}$ 1 e do not have a charge-transfer associated from the addenda to the magnetic ion as in the analogous Fe^{III} anion. As the values in Table 3 show the addition of one electron to the external site of the molecule yield almost insignificant changes in the inner tetrahedron. The reduction process involves the

Figure 5. Selected bond distances and net charges (in parentheses) computed for the fully oxidized anion $[SiW_{11}VO_{40}]^{5-}$.

transfer of only 0.05 e from XO_4 to the $W_{12}O_{36}$ cage in both ferromagnetic and antiferromagnetic states. The blue electron (α or β) is entirely localized on W's, each of which has a spin density of approximately 0.085 e, positive or negative depending on the nature of the coupling. Finally we should mention the alternative configuration of the reduced complex $[Co^IW_{12}O_{40}]^{7-}$. The formation of this species requires 0.78 eV more than the blue complex. This important energy arises from the high energy of the $33t_{2g}$ β orbital as mentioned above.

The Mixed Clusters $[SiM_{11}VO_{40}]^{5-}$ and Their Reduced Partners $[SiM_{11}VO_{40}]^{6-}$ (M = W and Mo). Complexes with the empirical formula $[XM_{12}O_{40}]^{n-}$ are a very small fraction of the number of POMs with the Keggin structure. Beyond the high symmetric anions there are complexes in which one MO_6 octahedron has been replaced by another octahedrally coordinated heteroatom such as $[XW_{11}Z(OH_2)O_{39}]^{n-}$ [53] or simply some of the M^{VI} metal is substituted by V.[54] Taking the oxidized cluster SiW_{12} as a point of departure, in this section we will analyze the changes induced in the POM when a tungsten is substituted by a vanadium. The distortion generated in the cluster by the metal substitution is essentially limited to the substituted MO_6 octahedron and related to the fact that V−O bond distances are shorter than W−O. Some selected bond lengths computed for the fully oxidized cluster $[SiW_{11}VO_{40}]^{5-}$ are given in Figure 5. Changes in the electronic properties are much more important. They are related to the set of occupied orbitals, such as the basicity of the external oxygen sites, but they also affect the lowest unoccupied orbitals, thus modifying the redox properties of the cluster. Population analysis shows that the changes predominantly take place in the addenda, which is now formally monoanionic. The net charge associated to the inner tetrahedron is −2.41 e, very similar to −2.59 e, the charge supported by SiO_4 in SiW_{12}. This suggests that the mixed cluster $[SiW_{11}VO_{40}]^{5-}$ may also be formulated as $SiO_4^{4-}@[W_{11}VO_{36}]^-$. The presence of a negative charge in the addenda $[W_{11}VO_{36}]^-$ could yield the false conclusion that the outer sphere in the mixed cluster

(51) Caballol, R.; Castell, O.; Illas, F.; Moreira, I. P. R.; Malrieu, J. P. *J. Phys. Chem. A* **1997**, *101*, 7860; Cabrero, J.; Ben Amor, N.; Graaf, C.; Illas, F.; Caballol, R. *J. Phys. Chem. A* **2000**, *104*, 9983.

(52) Illas, F.; Moreira, I. P. R.; Cohen G.; Barone, V. *Theor. Chem. Acc.* **2000**, *104*, 265 and references therein.
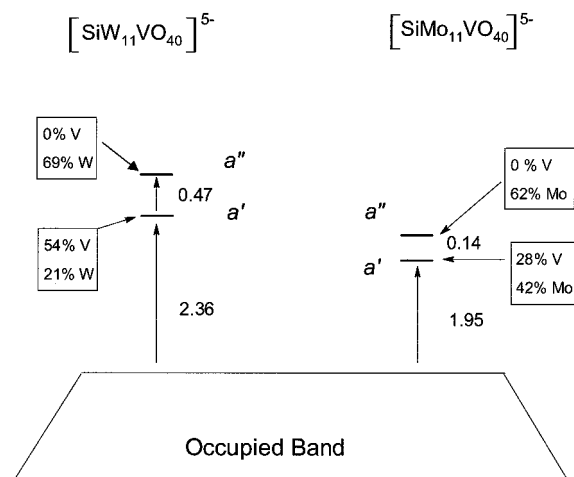
(53) Coronado, E.; Gómez-García, C. J. *Chem. Rev.* **1998**, *98*, 273.

(54) Courtin, P.; Chaveau F, Souchay, P. *C. R. Acad. Sci., Ser. C* **1964**, *258*, 1247; Souchay, P.; Bertho, G. *C. R. Acad. Sci., Ser. C* **1966**, *262*, 42; Courtin, P *Rev. Chim. Miner.* **1971**, *8*, 75, 221; Rabia, C.; Bettahar, M. M.; Launay, S.; Hervé, G.; Fournier, M. *J. Chim. Phys. Phys.-Chim. Biol.* **1995**, *92*, 1442; Smith, D. P.; Pope, M. T. *Inorg. Chem.* **1973**, *12*, 331; Tsigdinos, G. A.; Hallada, C. J. *Inorg. Chem.* **1968**, *7*, 437; Courtin, P. *Bull. Soc. Chim. Fr.* **1968**, 4799.

Figure 6. Orbital diagram for $[SiW_{11}VO_{40}]^{5-}$ and $[SiMo_{11}VO_{40}]^{5-}$ (energies in eV).

is much more basic than in the neutral cage. In fact, tungstens and the external oxygens only bonded to tungstens do not modify their populations when V is present in the addenda. However, the charge polarization in the VO_5 unit is much smaller due to the higher electronegativity of vanadium. Thus, whereas the charge for W's is +2.84 e, for V it is only +1.68 e. Oxygens connected to vanadium also support less charge; the computed charges for the terminal OV oxygen and OVW bridgings are −0.68 and −0.94 e, respectively, about −0.16 e less than the charges on the oxygen sites connected to tungstens (Figure 5). Similar differences have already been reported for the mixed Lindqvist structure $[V_2W_4O_{19}]^{4-}$ using the Hartree−Fock method and the topology of charge density analysis.[17b]

When the addenda contains only one V, as in $SiW_{11}V$, the molecule retains only one symmetry plane, and consequently the doubly degenerate LUMO in SiW_{12} now splits in two orbitals of symmetry a′ and a″. The orbital of symmetry a″ is very similar to its e precursor because it is delocalized over the tungstens. Orbital a′ is 0.47 eV lower in energy than a″ and is mainly localized on the vanadium center, although there is a small contribution of tungstens (Figure 6). The composition of these two orbitals opens up two possibilities for the one-electron reduced clusters: the formation of $SiW_{11}V^{IV}$ or the blue species $SiW_{11}V$ 1e. Calculations carried out for these two reduced anions indicate that the former configuration is the preferred one by 0.64 eV. This significant energy difference agrees with the observed magnetism for the reduced cluster, which is consistent with a localization of the metal electron.[46] The computed spin density confirms the distinct nature of the two states. In the lowest configuration, the spin density is 90% localized on V, the other 10% being delocalized over the tungstens. In contrast, in the first excited configuration the vanadium atom makes no contribution, and the spin density is more or less equally delocalized over all of the tungstens. Another evidence of localization of the extra electron into vanadium is the color of the anion, brown, typical of V(IV) in octahedral environments, instead of the expected blue color when delocalized electrons are present.

Let us now consider the analogous molybdenum vanadium cluster $[SiMo_{11}VO_{40}]^{5-}$. Here, the situation is somewhat different; since the d-molybdenum orbitals are lower in energy than tungsten orbitals, there is stronger competition between the molybdenum and vanadium orbitals. The two lowest metal orbitals for $[SiMo_{11}VO_{40}]^{5-}$ have a′ and a″ symmetries such as in the analogous tungsten system. This latter orbital is entirely

delocalized over molybdenums and is formally identical to the lowest metal a″ orbital found for $[SiW_{11}VO_{40}]^{5-}$. However, orbital a′, the LUMO in the fully oxidized anion, has a high participation of Mo orbitals (~42%), and the contribution of V orbitals lowers to ~28%. Moreover, because the molybdenum anions tend to have lower HOMO−LUMO energy gaps (Figure 3), the energy of the LUMO relative to the occupied band is 1.95 eV, 0.41 eV smaller than for the tungstate derivative. Another interesting feature of the molybdenum−vanadium mixed system is that the difference between the two lowest metal orbitals is only 0.14 eV. Almost the same energy difference (0.2 eV) was found between the two doublets of symmetries A′ and A″ in the reduced species, and is clearly lower than the energy computed for $[SiW_{11}VO_{40}]^{6-}$. Relative energies for orbitals a′ and a″ are given in Figure 6. When the metal electron is added to the orbital of symmetry a′, this mix with other orbitals of higher energies and increases the localization of the metal electron. Spin density analysis indicates that ~60% of the spin density is over the V center, and although this is a considerable percentage it is clearly lower than in the analogous tungstavanadate (~90%). In summary, the localized form is expected to dominate, but a thermodynamic mixture of the two species $SiMo_{11}V^{IV}$ and $SiMo_{11}V$ 1e cannot be ruled out for the reduced species. The tendency for metal electrons to localize in substituted Keggin structures was also observed by Bénard and co-workers for γ-$[SiW_{10}Mo_2S_2O_{38}]^{6-}$, a cluster with two metal electrons that are responsible for a relatively short Mo^V−Mo^V bond.[55] Finally, we should comment in relation to localized/delocalized states that whereas the HF method tends to favor overlocalized solutions the DFT approach favors the delocalization and therefore the degree of localization/delocalization of the metallic electrons in these compounds may depend on the used method.[56]

Conclusions and Summary

DFT calculations were carried out on a series of Keggin anions $[XM_{12}O_{40}]^{n-}$ where M = W or Mo and X is a main group element or a transition metal ion. The calculations support the hypothesis that an oxidized Keggin anion is a XO_4^{n-} clathrate inside a neutral $W_{12}O_{36}$ cage. The energy gap between the band of occupied orbitals, formally delocalized over the oxo ligands, and the unoccupied d-metal orbitals, delocalized over the addenda, is manifestly independent of the central ion. However, this energy gap relies heavily on the metal types in the addenda. Substitution of a W or a Mo by V produces important changes in the redox properties of the cluster. The LUMO in the oxidized species $SiW_{11}V$ is basically localized on the vanadium center which favors the formation of the reduced species $SiW_{11}V^{IV}$ and not the delocalized form $SiW_{11}V$ 1e, which is 0.64 eV less stable. Due to the low energy of the Mo orbitals the competition between the localized and delocalized forms is much more important, and the energy difference between them does not exceed 0.2 eV in the mixed molybdenum−vanadium derivative.

In agreement with the most recent structural characterization of $Co^{III}W_{12}$ the calculations predict a slight Jahn−Teller distortion for this complex. Calculations carried out on several configurations of $[CoW_{12}O_{40}]^{6-}$ show that the ground configuration corresponds to a Keggin structure with a Co^{II} as a central

(55) Romer, M.-M.; Bénard, M.; Secheresse F. In *Polyoxometalates: From Topology to Industrial Applications*; Pope, M. T., Müller, A., Eds.; Kluwer: Dordrecht, The Netherlands, in press.

(56) Picket, W. E. *Rev. Mod. Phys.* **1989**, *61*, 433; Illas, F.; Martin, R. *J. Chem. Phys.* **1998**, *108*, 2519; Martin R.; Illas, F. *Phys. Rev. Lett.* **1997**, *79*, 1539.

ion. The transformation of $Co^{II} \rightarrow Co^{III}$ by transferring one electron from cobalt to the sphere of tungstens requires ~1 eV. One-electron reduction of $Co^{II}W_{12}$ and $Fe^{III}W_{12}$ leads to the blue species $Co^{II}W_{12}$ 1e and $Fe^{III}W_{12}$ 1e, and no formation of $Co^{I}W_{12}$ and $Fe^{II}W_{12}$ is observed. It is easy to rationalize this fact if we take into account the high energy of unoccupied Fe and Co d-orbitals that should accommodate the additional electron in the reduced species. Present calculations also suggest that in heteropolytungstates it is more difficult to reduce $Co^{II} \rightarrow Co^{I}$ than $Fe^{III} \rightarrow Fe^{II}$, behavior that is well-known in basic inorganic chemistry. The blue species $Fe^{III}W_{12}$ 1e is notably antiferromagnetic, and in complete agreement with this behavior, the low spin state computed via a Broken-Symmetry approach is lower than the high-spin solution by 196 cm^{-1}. The LS state has a certain associated delocalization of the blue electron in the internal tetrahedron, which allows a small oxidation state reduction of iron. In contrast, $Co^{II}W_{12}$ 1e has a low ferromagnetic coupling and has no charge transfer between the two magnetic sides of the molecule. This blue species is 0.78 eV more stable than the alternative reduction product $Co^{I}W_{12}$.

JA003563J